Predicted kinetic behaviour of the oxidative degradation of organic pollutant using substituted MeCuFeO$_3$ (Me = Ca, Sr, CaSr) perovskite catalysts

Rasyidah Alrozi[1,2], Nor Aida Zubir [1,2*], Noor Fitrah Abu Bakar[3], Julius Motuzas[4], Noor Hana Hanif Abu Bakar[5], David Wang[6]

[1]*Chemical Engineering Studies, College of Engineering, Universiti Teknologi MARA, Cawangan Pulau Pinang, 13500, Permatang Pauh, Pulau Pinang, Malaysia*

[2]*Hybrid Nanomaterials, Interfaces & Simulation (HYMFAST), Chemical Engineering Studies, College of Engineering, Universiti Teknologi MARA, Cawangan Pulau Pinang, 13500, Permatang Pauh, Pulau Pinang, Malaysia*

[3]*School of Chemical Engineering, College of Engineering, Universiti Teknologi MARA Shah Alam, 40450, Shah Alam, Selangor, Malaysia*

[4]*The University of Queensland, FIM^{2}LAB-Functional Interfacial Materials and Membranes Laboratory, School of Chemical Engineering, Brisbane, Qld 4072, Australia*

[5]*Nanoscience Research Laboratory, School of Chemical Sciences, Universiti Sains Malaysia, 11800, Penang, Malaysia*

[6]*School of Chemical and Biomolecular Engineering, The University of Sydney, New South Wales, 2006, Australia*

ARTICLE INFO

ABSTRACT

The substitution of different types of A-site metal cations within the perovskite structure leads to a change in the catalytic activity of the resultant catalyst, which subsequently affects the overall kinetic behaviour of the degradation of organic pollutants. Hence, understanding the kinetics behaviour of the substituted perovskite catalysis is crucial for determining the reaction rates of the degradation process. This study investigates the catalytic performance and kinetic analysis of substituted MeCuFeO$_3$ (Me = Ca, Sr, CaSr) perovskite catalysts in the oxidation of organic pollutants, namely acid orange II (AOII) dye. The highest AOII degradation was achieved by CaCuFeO$_3$ (97 %) followed by CaSrCuFeO$_3$ (95 %) and SrCuFeO$_3$ (91 %) within 60 min of reaction in the presence of oxidant (H$_2$O$_2$). Interestingly, the AOII oxidation by CaCuFeO$_3$ followed a pseudo-second-order kinetic model while SrCuFeO$_3$ and CaSrCuFeO$_3$ were fitted to the BMG kinetic model. The reaction rate constant of CaCuFeO$_3$ (k = 1.9 × 10^{-2} L.mg^{-1}.min^{-1}) was higher by a magnitude of two and three than that of CaSrCuFeO$_3$ (k = 9.4 × 10^{-3} L.mg^{-1}.min^{-1}) and SrCuFeO$_3$ (k = 6.3 ×

[1]* Corresponding author. *E-mail address*: noraida709@uitm.edu.my

10^{-3} L.mg^{-1}.min^{-1}), respectively. These results indicate that the partial substitution of Sr in the A-site of CaCuFeO$_3$ leads to a slight deterioration in the overall catalytic performance of the oxidative degradation of AOII, which contributes to a change in the behaviour of the reaction kinetic models.

1. INTRODUCTION

Organic pollutants, such as dyes, are widely used in various industries including textile, cosmetics, paper, paint, pharmaceutical, plastic, leather, and food. About 700,000 metric tonnes of synthetic dyes are produced yearly, with more than 10,000 commercial dyes used by textile industries [1]. Textile dyes exhibit weak binding affinity to the fabric and are released as effluent into the water bodies [2]. Therefore, improper disposal of dye-containing wastewater can lead to serious environmental contamination, particularly water pollution. The untreated dye-containing wastewater poses severe risks to the natural environment and public health, as the dyes are known to have plausible toxic, carcinogenic and mutagenic impacts on aquatic ecosystems. Hence, proper treatment of dye-containing wastewater prior to direct discharge to main water bodies is essential.

Physical, chemical, and biological treatment techniques [3–8] are the most widely utilized wastewater treatment technology. The physical treatments such as adsorption, coagulation-flocculation, and membrane filtration are ineffective in eliminating all recalcitrant organic pollutants from the water bodies because these methods are impacted by secondary contamination, which requires additional post-treatment process [8]. Biological treatments, on the other hand, need a considerable amount of land and longer biological reaction times. For instance, microorganisms like algae, fungi, enzymes, and bacteria typically require long digestion periods to effectively decompose organic pollutants and are sensitive to hazardous substances [6]. Chemical treatments, namely advanced oxidation processes (AOPs), have garnered significant interest in recent years due to the strong oxidation ability to effectively decompose recalcitrant organic pollutants non-selectively, whilst minimizing the generation of secondary pollutants [5]. Among the available AOPs, the Fenton reaction has become the most popular technique for treating organic wastewater [6–8]. The conventional Fenton oxidation process includes the catalytic activation of hydrogen peroxide (H$_2$O$_2$) by ferrous ions (Fe^{2+}) to generate hydroxyl (HO•) radicals [9]. Efficient generation of HO• radicals during catalysis is important due to their inherent non-selective nature with strong oxidizing capabilities (E°=2.8 V) to effectively degrade the organic pollutants. However, the classical Fenton method has drawbacks, including a limited pH range, forming a large volume of iron sludge, which needs a secondary post-treatment process, and difficulties in catalyst recovery [10]. To overcome these limitations, the heterogeneous Fenton-like oxidation process was introduced, and extensive research is focusing on the development of highly efficient solid catalysts.

Recently, perovskites have emerged as promising materials for heterogeneous catalytic applications in the degradation of recalcitrant organic pollutants. Perovskites (ABO$_3$) are ceramic materials with a cubic structure, where the cation sites (A or B) can be partially substituted with other cations (A' and/or B'). This substitution leads to the formation of ternary (AA'BO or ABB'O) or quaternary (AA'BB'O) types of perovskite compounds. The selection of cation being substituted into the perovskite structure can significantly influence the overall catalytic activity of resultant catalyst in degrading organic pollutants in wastewater. The improved overall oxidative catalytic performance can be attributed to the effective generation of highly reactive radical species (HO• radicals) during heterogeneous catalysis [11].

Various types of rare earths or alkaline earth elements can serve as substitution cations at the A-site [12–15], as well as transition metals at the B-site [16-17]. A recent report revealed that substitution of Sr as A-site cation lead to superior catalytic activity of La$_{0.5}$Sr$_{0.5}$Mn$_{0.5}$Fe$_{0.5}$O$_{2.92}$ in degrading rhodamine B dye

(99 % degradation in 25 min, k = 0.1710 min^{-1}), compared to Ca substitution (La$_{0.5}$Ca$_{0.5}$Mn$_{0.5}$Fe$_{0.5}$O$_{2.92}$, 99 % degradation in 45 min, k = 0.0828 min^{-1}) [12]. Once the Sr was substituted into the La$_{0.5}$Mn$_{0.5}$Fe$_{0.5}$O$_{2.92}$ perovskite structure, the overall reaction rate improved almost twofold compared to Ca. Moreover, Cheng et al. [13] discovered that partial substitution of Sr in the A-site of LaFeO$_3$ enhanced 2,4-dichlorophenoxyacetic acid degradation efficiency by 80 %, with the reaction rate constant (k = 0.0720 min^{-1}) being 5.7 times higher than the LaFeO$_3$. Further, Wang et al. [14] reported that degradation of ciprofloxacin boosted by 75 % within 60 min of reaction after BiFeO$_3$ was partially substituted with Sr. The reaction rate constant of Bi$_{0.9}$Sr$_{0.1}$FeO$_3$ (k = 0.0935 min^{-1}) was increased by a magnitude of twenty-four as compared to the BiFO$_3$. On the contrary, in the A-site of Ca$_x$Sr$_{1-x}$CuO$_{3-\delta}$ perovskite structure, Chen et al. [15] found that sample catalysts with a higher Ca content (x= 0.75 and 1, ~95 % in 60 min) exhibited a slightly higher orange II dye degradation than samples with a high Sr content (x= 0 and 0.25, ~90 % in 60 min). The reported studies demonstrate the efficient degradation of recalcitrant organic contaminants in wastewater by ternary or quaternary perovskite compounds.

Based on the reviewed literature [12–15], most of the A-site substituted perovskite catalysts followed the pseudo-first-order reaction kinetic model. However, due to the contradictory findings on the effects of Sr and Ca substitution on the overall catalytic activity of resultant catalysts at room temperature heterogeneous Fenton-like oxidation catalysis [12–15], it is important to evaluate the influence of the partial or complete substitution of the A-site cation within the perovskite structure on the reaction rate constants of the recalcitrant organic pollutants' degradation using a different set of kinetic models. In-depth analysis of kinetic models on a laboratory scale is important for scale-up, reactor design, and optimization of reaction performance.

Herein, we evaluate the kinetic behaviour of A-site substituted MeCuFeO$_3$ (Me = Ca, Sr, CaSr) perovskite catalysts in the oxidation of organic pollutants at room temperature using different kinetic models (pseudo-zero-order, first-order, second-order and BMG-Behnajady, Modirshahla, and Ghanbary). Acid orange II (AOII) dye was selected as the model organic pollutant due to its representation of 15% of global dye output [18] and the most frequently discharged dye from textile production [15]. The catalytic activity and reaction kinetic models of MeCuFeO$_3$ (Me = Ca, Sr, CaSr) perovskite catalysts on AOII degradation in the presence of oxidant were discussed in this study.

2. METHODOLOGY

2.1 Materials

Calcium nitrate tetrahydrate (Ca(NO$_3$)$_2$.4H$_2$O; ≥99 %), copper(II) nitrate trihydrate (Cu(NO$_3$)$_2$.2.5H$_2$O; ≥99 %), iron(III) nitrate nonahydrate (Fe(NO$_3$)$_3$.9H$_2$O; 99 %), strontium nitrate Sr(NO$_3$)$_2$, ethylenediaminetetraacetic acid (EDTA), ammonium hydroxide (NH$_4$OH) solution, hydrogen peroxide (H$_2$O$_2$; 30 % (w/w)), and acid orange II (AOII) were supplied by Sigma Aldrich. Citric acid monohydrate (C$_6$H$_8$O$_7$.H$_2$O; ≥99 %) was purchased from QReC (Asia). All chemicals were of analytical grade and used as received without further purification.

2.2 Synthesis of MeCuFeO3 (Me = Ca, Sr, CaSr) perovskite catalysts

The synthesis of MeCuFeO$_3$ (Me = Ca, Sr, CaSr) perovskite catalysts was carried out using EDTA-citric acid complexation method. Each A/B-site cation molar concentration was fixed at 0.05 M. A set of molar ratios of A-site precursor: A'-site precursor: B-site precursor: B'site precursor: ethylenediaminetetraacetic acid (EDTA): citric acid: ammonium hydroxide was kept constant at 1:1:1:1:1.1:2:10.

For instance, in the synthesis of $CaCuFeO_3$ catalyst, 0.05 M $Ca(NO_3)2.4H_2O$, 0.05 M $Cu(NO_3)2.2.5H_2O$, 0.05 M $Fe(NO_3)_3.9H_2O$, and 0.1 M $C_6H_8O_7.H_2O$ solutions was mixed and stirred for 15 min at the beginning. Then, a solution mixture containing 0.055 M EDTA and 0.05 M NH_4OH was added to the former mixture and stirred for 15 min at room temperature until well mixed.

Subsequently, the resultant homogeneous mixture was heated at 100 ℃ under stirring to evaporate water to form a viscous solution. Further gelation of the viscous solution was carried out in the oven at 90 ℃ for 24 hr. The dried gel samples underwent a two-stage sintering process in a muffle furnace: the first stage at 450 ℃ for 8 hr and the second stage at 800 ℃ for 4 hr at a ramping rate of 5 ℃ min^{-1} in air. The resultant $CaCuFeO_3$ was ground and stored prior to further use. Analogous procedures were repeated for different substituted perovskite catalysts using strontium to synthesize $SrCuFeO_3$ and $CaSrCuFeO_3$, respectively.

2.3 Catalytic performances

The catalytic activity of the $MeCuFeO_3$ (Me = Ca, Sr, CaSr) perovskite catalysts was investigated in oxidative degradation of AOII (35 mg L^{-1}) by dispersing 0.1 g catalyst in 100 mL of AOII solution at room temperature. The reaction was initiated by dispensing 22 mM of H_2O_2 into the reaction mixture and stirring at 200 rpm for 90 min. Approximately 3 mL of the reaction suspension was withdrawn and filtered at regular intervals through a 0.2 μm filter syringe. The concentration of AOII was determined by measuring the absorbance of the sample solution at λ_{max} of 486 nm using a UV-vis spectrophotometer (Perkin Elmer, Lambda 25). The percentage of AOII degradation was calculated by following Eq. (1).

$$\text{Percentage of AOII degradation} = \frac{C_o - C_t}{C_o} x\,100 \tag{1}$$

where C_o is the initial concentration of AOII (mg L^{-1}), and C_t is the final concentration at a specific reaction time (mg L^{-1}). Similar procedures were repeated in the absence of H_2O_2 while dispersing the catalyst in the solution mixture for validation of the adsorption process. The experiments were consistently reproducible with a standard deviation of less than 5%.

2.4 Reaction kinetic analysis

The oxidative degradation of AOII in the presence of $MeCuFeO_3$ (Me = Ca, Sr, CaSr) perovskite catalysts were evaluated using the zero-order, first-order, second-order and BMG-Behnajady, Modirshahla, and Ghanbary [19] kinetic models. The zero-order, first-order, and second-order kinetic models are expressed by Eqs. (2)-(4), accordingly.

$$C_t = C_o - k_o t \tag{2}$$

$$\ln C_t = \ln C_o - k_1 t \tag{3}$$

$$\frac{1}{C_t} = \frac{1}{C_o} + k_2 t \tag{4}$$

2.5 Reaction kinetic analysis

The oxidative degradation of AOII in the presence of MeCuFeO$_3$ (Me = Ca, Sr, CaSr) perovskite catalysts were evaluated using the zero-order, first-order, second-order and BMG-Behnajady, Modirshahla, and Ghanbary [19] kinetic models. The zero-order, first-order, and second-order kinetic models are expressed by Eqs. (2)-(4), accordingly.

The k_o (mg L^{-1} min^{-1}), k_1 (min^{-1}), and k_2 (L mg^{-1} min^{-1}) are apparent kinetic rate constants of zero-order, first-order, and second-order models, respectively. Meanwhile t is reaction time, and C_t is AOII concentration at a given time t. The BMG model is defined by Eq. (5) [19]:

$$\frac{t}{\left[1-\left(\frac{C_t}{C_o}\right)\right]} = m + bt \tag{5}$$

The physical interpretations of the m and b can be demonstrated by modifying Eq. (5) and substituting these two constants for t in two distinct scenarios: (i) at the initial of the reaction (when $t = 0$) and (ii) as the reaction progresses towards its completion (when t is quite large) [20], which results to Eq. (6) and Eq. (7) [21], respectively.

$$\frac{dC}{dt} = -C_0\left(\frac{1}{m}\right) \text{ at } t = 0 \tag{6}$$

$$C = C_0\left(1-\frac{1}{b}\right) \text{ at very large } t \tag{7}$$

Eq. (6) can be compared with the design equation of a constant-density batch reactor at $t = 0$ *(dC/dT = r$_0$; t = 0)*. Hence, *1/m* represents the initial degradation rate *(-r$_0$)*, specifically expressed as *-r$_0$ = C$_o$(1/m)*. Meanwhile, Eq. (7) can be compared with the conversion equation in a constant-density batch reactor, *X = (C$_0$ - C)/C* or *C = C$_0$ (1 − X)*. From this equation, *1/b* is defined as the maximum possible conversion that might have been obtained following an extremely lengthy or infinite reaction time, which is referred to as the maximum oxidation capacity [21-22].

3. RESULTS AND DISCUSSION

3.1 Catalytic performances

Heterogeneous Fenton-like reaction involved with concurrent adsorption and reaction processes at the solid-liquid interfaces of the resultant catalyst during catalysis. Therefore, the dominancy of either one of the two processes is important to be assessed during the catalysis. Fig. 1 shows the adsorption profile of MeCuFeO$_3$ (Me = Ca, Sr, CaSr) perovskite catalysts in the absence of H$_2$O$_2$. The adsorption capacities of CaCuFeO$_3$, SrCuFeO$_3$ and CaSrCuFeO$_3$ perovskite for AOII removal were 28 %, 35 % and 32 % within 60 min, respectively. At 90 min, all catalysts reached saturation adsorption of nearly 35 %. The limited adsorption of all the resultant perovskite catalysts on AOII can be attributed to the significant repulsion between the negatively charged perovskite catalyst and the anionic AOII [22]. Besides, the non-porous characteristics of the perovskite materials [15, 25–28] could hinder the preferential adsorption and solid-liquid contact between the catalysts and the AOII solution.
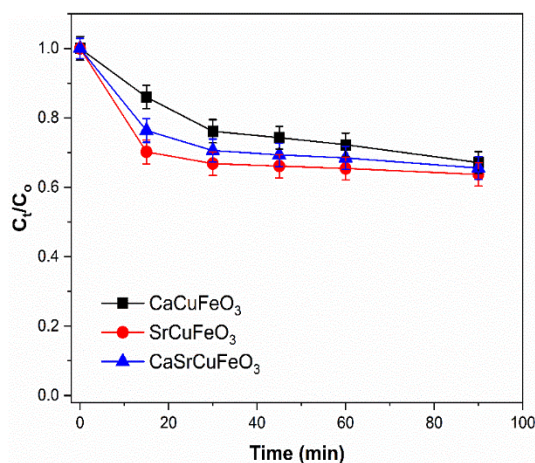
Fig. 1. Adsorption profile of AOII solution using different substituted $MeCuFeO_3$ (Me = Ca, Sr, CaSr) perovskite catalysts. Experimental conditions: AOII = 35 mg L^{-1}; catalyst = 1.0 g L^{-1}; unadjusted pH and room temperature.

Fig. 2 shows the overall AOII's degradation profile of heterogeneous Fenton-like oxidation in the presence of $MeCuFeO_3$ (Me = Ca, Sr, CaSr) perovskite catalysts and H_2O_2 as an oxidant. Significant degradation of AOII was observed within 90 min of the reaction in the presence of both substituted A-site perovskite catalysts and H_2O_2. Meanwhile, nearly no AOII degradation was observed in the presence of H_2O_2 alone. Such findings reveal that H_2O_2 is essentially unable to oxidise AOII degradation without the presence of a catalyst.

The rate of AOII degradation can be well represented by the sequence of catalytic reactivity of substituted A-site catalysts, which are as follows: $CaCuFeO_3$ > $CaSrCuFeO_3$ > $SrCuFeO_3$. The AOII degradation efficiency for $CaCuFeO_3$ (97 %) was higher than $SrCuFeO_3$ (91 %), which might be attributed to the more formation of HO• radicals in the presence of Ca cation at the A-site compared to Sr cation. On the other hand, when Ca was partially substituted by Sr in $CaCuFeO_3$, a rapid degradation rate of AOII was observed in the first 15 min but then the reaction slowed down and reached 95 % degradation after 60 min which is 2 % lower than the $CaCuFeO_3$. The small differences in catalytic performances between the ternary $CaCuFeO_3$ and quaternary $CaSrCuFeO_3$ perovskite catalyst suggest that partial substitution of Sr in the A-site of $CaCuFeO_3$ did not significantly improve the overall catalytic performance. Similar findings have also been observed for AOII degradation using $CaCuO_3$ and $Ca_{0.5}Sr_{0.5}CuO_{3-\delta}$, where degradation efficiency obtained was 95 % and 90 %, respectively [15].

The degradation of the AOII dye was confirmed by the decrease in absorbance intensity in the UV-Vis spectrum of AOII at a maximum wavelength of 486 nm, as shown in Fig. 3. A significant absorption peak reduction at 486 nm was observed after undergoing 90 min of reaction in the presence of A-site substituted perovskite catalyst. Such findings confer the ability of perovskite catalyst in activating the H_2O_2 into HO• radicals. The efficient generation of HO• radicals enable the destruction of hydrazone bonds within the molecular structure of AOII during catalysis. The degradation of the AOII structure can be further supported by the significant decrease of absorption peaks of 430 nm and 310 nm, which are attributed to the azo and naphthalene structures [27].

3.2 Reaction kinetic analysis

The kinetic behavior of AOII oxidation by $MeCuFeO_3$ (Me = Ca, Sr, CaSr) perovskite catalysts in the presence of H_2O_2 were further evaluated by four kinetic models (pseudo-zero-order (Fig. 4a), first-order (Fig. 4b), second-order (Fig. 4c) and BMG (Fig. 4d). The results of correlation coefficients (R^2), apparent

kinetic constants of the pseudo-zero-order, first-order, second-order (k_o, k_1 and k_2) and parameters obtained on the BMG model (*1/m* and *1/b*) by MeCuFeO$_3$ (Me = Ca, Sr, CaSr) in the presence of H$_2$O$_2$ for AOII oxidation are shown in Table 1. As observed in Table 1, the pseudo-second order kinetic model fitted well to the AOII oxidation by CaCuFeO$_3$ perovskite catalysts, as it obtained higher R^2 values than zero-order, first-order and BMG kinetic models. This result implies that the concentration of AOII and oxidant (H$_2$O$_2$) affect the catalytic reaction of CaCuFeO$_3$. Further, the pseudo-second-order reaction kinetics was found to be the most suitable model for elucidating Fe^{3+}-containing processes, wherein the reaction represents a single degradation stage [28]. From Fig. 4c, CaCuFeO$_3$ exhibited the highest slope for the second-order reaction kinetics, showing an increase in the values of k$_2$ (Table 1). The reaction rate constant of CaCuFeO$_3$ (k = 1.9 x 10^{-2} L.mg^{-1}.min^{-1}) was higher by a magnitude of two and three than that of CaSrCuFeO$_3$ (k = 9.4 x 10^{-3} L.mg^{-1}.min^{-1}) and SrCuFeO$_3$ (k = 6.3 x 10^{-3} L.mg^{-1}.min^{-1}), respectively.

On the contrary, the AOII oxidation by SrCuFeO$_3$ and CaSrCuFeO$_3$ were fitted to the BMG kinetic model (R^2 > 0.96) (Table 1 and Fig. 4b). The BMG kinetic model may represent the attributes of the Fe^{2+}/H$_2$O$_2$ system via the Fenton process, which follows a two-stage pattern. This pattern consists of an initial rapid stage, followed by a slower stage. The rapid stage corresponds to the interaction between Fe^{2+} and H$_2$O$_2$, whereas the slower stage is explained by the accumulation of Fe^{3+} and a restricted regeneration of Fe^{2+} by H$_2$O$_2$ [23,30,31]. This behavior is in line with the AOII oxidation profiling pattern for CaSrCuFeO$_3$ (Fig. 2), as previously discussed, where a rapid degradation rate of AOII was observed for the first 15 min and then followed by a slow reaction afterwards. In fact, based on the parameter *1/m* (initial degradation rate) obtained from the BMG model (Table 1), the presence of CaSrCuFeO$_3$ in the reaction medium exhibited the highest initial degradation rate (1/m = 4.7058), which implied a higher AOII degradation rate during the early stage of catalysis compared to SrCuFeO$_3$.
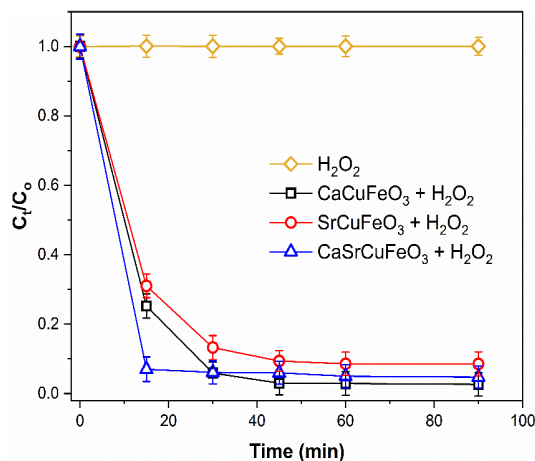

Fig. 2. Degradation profile of AOII solution in heterogeneous Fenton-like reaction using different substituted MeCuFeO$_3$ (Me = Ca, Sr, CaSr) perovskite catalysts. Experimental conditions: AOII = 35 mg L^{-1}; H$_2$O$_2$ = 22 mM; Catalyst = 1.0 g L^{-1}; room temperature and unadjusted pH

On the contrary, when examining the parameter 1/b (maximum oxidation capacity) (Table 1), it is evident that CaCuFeO$_3$ exhibits the highest value (1/b = 1.0004), followed by CaSrCuFeO$_3$ (1/b = 0.9490) and SrCuFeO$_3$ (1/b = 0.9413). This observation is further supported by the total AOII degradation efficiency after 60 minutes (Fig. 2). These results are in agreement with prior studies [32–37], underscoring the suitability of the BMG model for characterizing the degradation of organic pollutants through AOPs.
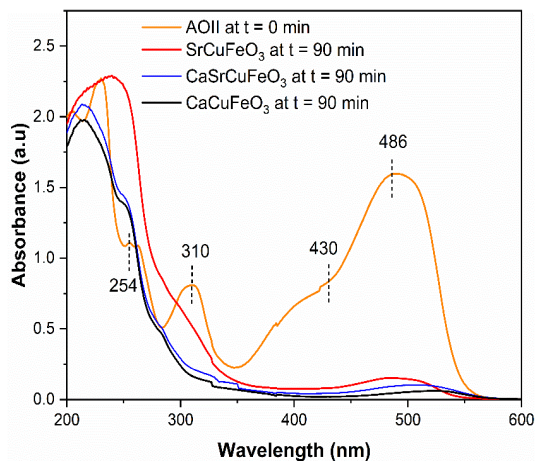
Fig. 3. UV–vis spectra of AOII at different reaction times in the presence of substituted MeCuFeO₃ (Me = Ca, Sr, CaSr) perovskite catalysts and H₂O₂. Experimental conditions: AOII = 35 mg L⁻¹; H₂O₂ = 22 mM; Catalyst = 1.0 g L⁻¹; room temperature and unadjusted pH
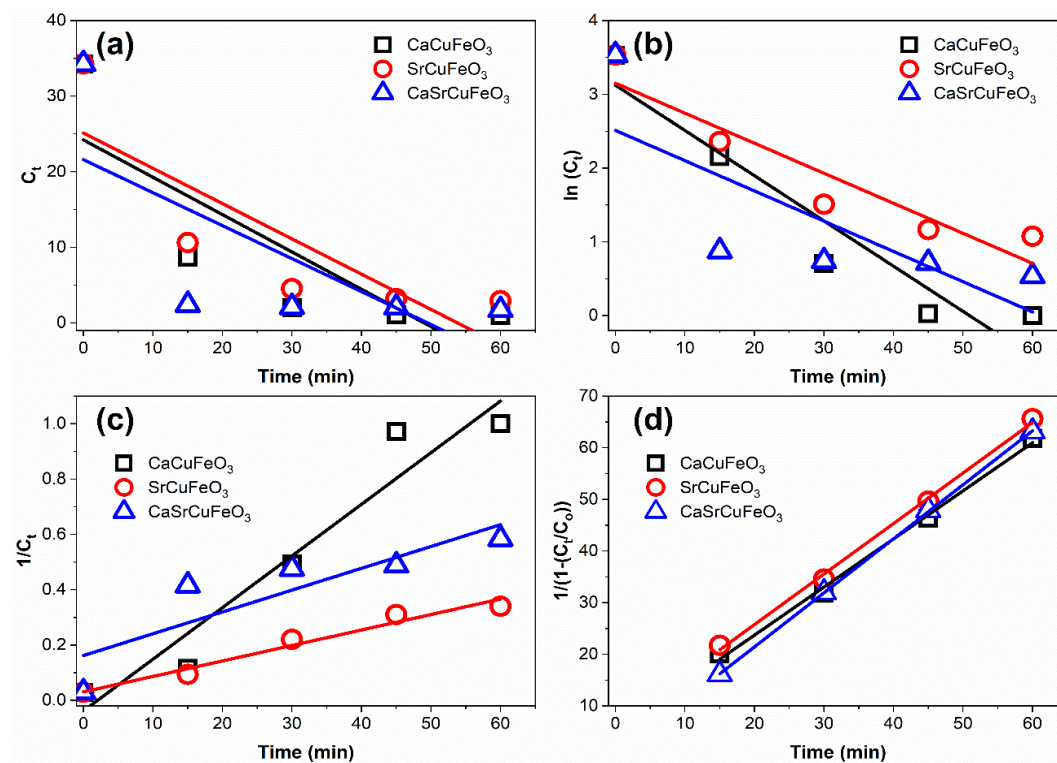

Fig. 4. AOII oxidation by different substituted MeCuFeO₃ (Me = Ca, Sr, CaSr) perovskite catalysts using (a) zero-order, (b) first-order, (c) second-order and (d) BMG kinetic model. Experimental conditions: AOII = 35 mg L⁻¹; H₂O₂ = 22 mM; Catalyst = 1.0 g L⁻¹; room temperature and unadjusted pH

Table 1. Apparent kinetic rate constants of the zero-order (k_0), first-order (k_1), and second-order (k_2), parameters obtained on the BMG model (*1/m* and *1/b*) and correlation coefficients (R^2) by $MeCuFeO_3$ (Me = Ca, Sr, CaSr) in the presence of H_2O_2 after data fits for AOII oxidation (60 min)

Catalyst	Zero Order		First Order		Second Order		BMG		
	k_o (mg L^{-1} min^{-1})	R^2	k_1 (min^{-1})	R^2	k_2 (L mg^{-1} min^{-1})	R^2	*1/m* (min^{-1})	*1/b*	R^2
$CaCuFeO_3$	0.4942	0.6755	0.0613	0.9012	0.0192	0.9254	0.4901	1.0004	0.9236
$SrCuFeO_3$	0.4671	0.6925	0.0061	0.6333	0.0063	0.9573	0.4021	0.9413	0.9629
$CaSrCuFeO_3$	0.4365	0.5164	0.0572	0.6450	0.0094	0.7539	4.7058	0.9490	0.9799

4. CONCLUSION

In this study, the reactivity and kinetic behavior of $MeCuFeO_3$ (Me = Ca, Sr, CaSr) perovskite catalysts in the oxidation of AOII were investigated. $CaCuFeO_3$ achieved the maximum degradation of AOII at 97 %, followed by $CaSrCuFeO_3$ at 95 % and $SrCuFeO_3$ at 91 %, within 60 min of reaction time in the presence of H_2O_2. The AOII oxidation by $CaCuFeO_3$ fitted a pseudo-second-order kinetic model whereas $SrCuFeO_3$ and $CaSrCuFeO_3$ were better described by the BMG kinetic model. The order of reaction rate constant was found to be in the sequence of $CaCuFeO_3$ (k = 1.9 x 10^{-2} L.mg^{-1}.min^{-1}) > $CaSrCuFeO_3$ (k = 9.4 x 10^{-3} L.mg^{-1}.min^{-1}) > $SrCuFeO_3$ (k = 6.3 x 10^{-3} L.mg^{-1}.min^{-1}). The results suggest that partial substitution of Sr in the A-site of $CaCuFeO_3$ during the oxidative degradation of AOII did not significantly affect the overall catalytic performance.

5. ACKNOWLEDGEMENT

6. CONFLICT OF INTEREST

The authors affirm that there is no conflict of interest pertaining to the publication of this paper.

7. AUTHORS' CONTRIBUTIONS

Rasyidah Alrozi: Material preparation, data collection, analysis and writing-original draft; **Nor Aida Zubir**: Supervision, conceptualisation, methodology, resource, analysis, validation, writing-review and editing; **Noor Fitrah Abu Bakar**: Validation, writing-review and editing; **Julius Motuzas**: Validation, writing-review and editing; **Noor Hana Hanif Abu Bakar**: Validation, writing-review and editing.

8. REFERENCES

[1]   V. Chandanshive, S. Kadam, N. Rane, B. Jeon, J. Jadhav, and S. Govindwar, "In situ textile wastewater treatment in high rate transpiration system furrows planted with aquatic macrophytes and floating phytobeds," *Chemosphere*, vol. 252, p. 126513, 2020. Available: doi: 10.1016/j.chemosphere.2020.126513.

[2]   R. Al-Tohamy *et al.*, "A critical review on the treatment of dye-containing wastewater: Ecotoxicological and health concerns of textile dyes and possible remediation approaches for environmental safety," *Ecotoxicol. Environ. Saf.*, vol. 231, p. 113160, 2022. Available: doi: 10.1016/j.ecoenv.2021.113160.

[3]   S. K. Kamal and A. S. Abbas, "Fenton oxidation reaction for removing organic contaminants in synesthetic refinery wastewater using heterogeneous Fe-Zeolite : An experimental study , optimization , and simulation," *Case Stud. Chem. Environ. Eng.*, vol. 8, p. 100458, 2023. Available: doi: 10.1016/j.cscee.2023.100458.

[4]   R. Pelalak, A. Hassani, Z. Heidari, and M. Zhou, "State-of-the-art recent applications of layered double hydroxides (LDHs) material in Fenton-based oxidation processes for water and wastewater treatment," *Chem. Eng. J.*, vol. 474, p. 145511, 2023. Available: doi: 10.1016/j.cej.2023.145511.

[5]   H. Liu, X. Li, X. Zhang, F. Coulon, and C. Wang, "Harnessing the power of natural minerals: A comprehensive review of their application as heterogeneous catalysts in advanced oxidation processes for organic pollutant degradation," *Chemosphere*, vol. 337, no. June, p. 139404, 2023. Available: doi: 10.1016/j.chemosphere.2023.139404.

[6]   M. F. Hanafi and N. Sapawe, "A review on the current techniques and technologies of organic pollutants removal from water/wastewater," *Mater. Today Proc.*, vol. 31, no. 2020, pp. A158–A165, 2021. Available: doi: 10.1016/j.matpr.2021.01.265.

[7]   M. Zhang, H. Dong, L. Zhao, D. Wang, and D. Meng, "A review on Fenton process for organic wastewater treatment based on optimization perspective," *Sci. Total Environ.*, vol. 670, pp. 110–121, 2019. Available: doi: 10.1016/j.scitotenv.2019.03.180.

[8]   M. Bartolomeu, M. G. P. M. S. Neves, M. A. F. Faustino, and A. Almeida, "Wastewater chemical contaminants: remediation by Advanced Oxidation Processes," *Photochem. Photobiol. Sci.*, vol. 17, pp. 1573–1598, 2018. Available: doi: 10.1039/C8PP00249E.

[9]   H. Yu, J. Ji, Q. Yan, and M. Xing, "Transition metal phosphides for heterogeneous Fenton-like oxidation of contaminants in water," *Chem. Eng. J.*, vol. 449, p. 137856, 2022. Available: doi: 10.1016/j.cej.2022.137856.

[10]   N. Li *et al.*, "H2O2 activation and contaminants removal in heterogeneous Fenton-like systems," *J. Hazard. Mater.*, vol. 458, p. 131926, 2023. Available: doi: 10.1016/j.jhazmat.2023.131926.

[11]   N. N. A. Abdul Rahman *et al.*, "B-site Substitution Effects on the Catalytic Activity of Perovskites Compounds towards Oxidative Degradation of Orange II Solutions," *IOP Conf. Ser. Mater. Sci. Eng.*, vol. 864, no. 1, 2020. Available: doi: 10.1088/1757-899X/864/1/012001.

[12]   S. Sharma, U. Manhas, I. Qadir, A. K. Atri, S. Singh, and D. Singh, "A comparative study of structural, magnetic and catalytic properties of half doped nanocrystalline La0.5A0.5Mn0.5Fe0.5O3 (A = Ca, Sr) perovskite oxides: Highly efficient and versatile candidates for enhanced oxidative degradation of hazardous organic dyes," *Mater. Chem. Phys.*, vol. 306, no. June, p. 128033, 2023. Available: doi: 10.1016/j.matchemphys.2023.128033.

[13]   C. Cheng, S. Gao, J. Zhu, G. Wang, L. Wang, and X. Xia, "Enhanced performance of LaFeO3 perovskite for peroxymonosulfate activation through strontium doping towards 2,4-D degradation," *Chem. Eng. J.*, vol. 384, no. October 2019, p. 123377, 2020. Available: doi: 10.1016/j.cej.2019.123377.

[14]   C. Wang, S. Gao, J. Zhu, X. Xia, M. Wang, and Y. Xiong, "Enhanced activation of peroxydisulfate by strontium modified BiFeO3perovskite for ciprofloxacin degradation," *J. Environ. Sci. (China)*, vol. 99, pp. 249–259, 2021. Available: doi: 10.1016/j.jes.2020.04.026.

[15]   H. Chen, J. Motuzas, W. Martens, and J. C. Diniz da Costa, "Degradation of azo dye Orange II under dark ambient conditions by calcium strontium copper perovskite," *Appl. Catal. B Environ.*, vol. 221, no. April 2017, pp. 691–700, 2018. Available: doi: 10.1016/j.apcatb.2017.09.056.

[16]   L. Xie *et al.*, "Enhanced redox activity and oxygen vacancies of perovskite triggered by copper incorporation for the improvement of electro-Fenton activity," *Chem. Eng. J.*, vol. 428, no. July 2021, p. 131352, 2022. Available: doi: 10.1016/j.cej.2021.131352.

[17]   K. Pan *et al.*, "Oxygen vacancy mediated surface charge redistribution of Cu-substituted LaFeO3 for degradation of bisphenol A by efficient decomposition of H2O2," *J. Hazard. Mater.*, vol. 389, no. January, p. 122072, 2020. Available: doi: 10.1016/j.jhazmat.2020.122072.

[18]   N. Riaz, F. K. Chong, B. K. Dutta, Z. B. Man, M. S. Khan, and E. Nurlaela, "Photodegradation of Orange II under visible light using Cu-Ni/TiO 2: Effect of calcination temperature," *Chem. Eng. J.*, vol. 185–186, pp. 108–119, 2012. Available: doi: 10.1016/j.cej.2012.01.052.

[19]   M. A. Behnajady, N. Modirshahla, and F. Ghanbary, "A kinetic model for the decolorization of C.I. Acid Yellow 23 by Fenton process," *J. Hazard. Mater.*, vol. 148, no. 1–2, pp. 98–102, 2007. Available: doi: 10.1016/j.jhazmat.2007.02.003.

[20]   S. Haji, M. Khalaf, M. Shukrallah, J. Abdullah, and S. Ahmed, "A kinetic comparative study of azo dye decolorization by catalytic wet peroxide oxidation using Fe–Y zeolite/H2O2 and photooxidation using UV/H2O2," *React. Kinet. Mech. Catal.*, vol. 114, no. 2, pp. 795–815, 2015. Available: doi: 10.1007/s11144-014-0810-3.

[21]   C. S. Santana, M. D. Nicodemos Ramos, C. C. Vieira Velloso, and A. Aguiar, "Kinetic Evaluation of Dye Decolorization by Fenton Processes in the Presence of 3-Hydroxyanthranilic Acid," *Int. J. Environ. Res. Public Health*, vol. 16, p. 1602, 2019.

[22]   R. Alrozi *et al.*, "Functional role of B-site substitution on the reactivity of CaMFeO3 (M = Cu, Mo, Co) perovskite catalysts in heterogeneous Fenton-like degradation of organic pollutant," *J. Taiwan Inst. Chem. Eng.*, vol. 143, no. January, p. 104675, 2023.

[23]   H. Chen, J. Motuzas, W. Martens, and J. C. Diniz da Costa, "Surface and catalytic properties of stable Me(Ba, Ca and Mg)SrCoO for the degradation of orange II dye under dark conditions," *Appl. Surf. Sci.*, vol. 450, pp. 292–300, 2018. Available: doi: 10.1016/j.apsusc.2018.04.193.

[24]   H. Chen, J. Motuzas, W. Martens, and J. C. Diniz da Costa, "Ceramic metal oxides with Ni2+ active phase for the fast degradation of Orange II dye under dark ambiance," *Ceram. Int.*, vol. 44, no. 6, pp. 6634–6640, 2018. Available: doi: 10.1016/j.ceramint.2018.01.071.

[25]   H. Chen, J. Motuzas, W. Martens, and J. C. Diniz Da Costa, "Effective degradation of azo dyes in the dark by Cu2+ active sites in CaSrNiCu oxides," *J. Environ. Chem. Eng.*, vol. 6, no. 5, pp. 5870–5878, 2018. Available: doi: 10.1016/j.jece.2018.08.060.

[26]   H. Chen, J. Motuzas, W. Martens, and J. C. Diniz da Costa, "Degradation of orange II dye under dark ambient conditions by MeSrCuO (Me = Mg and Ce) metal oxides," *Sep. Purif. Technol.*, vol. 205, no. May, pp. 293–301, 2018. Available: doi: 10.1016/j.seppur.2018.05.029.

[27]   P. Ji, J. Zhang, F. Chen, and M. Anpo, "Study of adsorption and degradation of acid orange 7 on the surface of CeO2 under visible light irradiation," *Appl. Catal. B Environ.*, vol. 85, no. 3–4, pp. 148–154, 2009. Available: doi: 10.1016/j.apcatb.2008.07.004.

[28]   C. S. Santana and A. Aguiar, "Effect of biological mediator, 3-hydroxyanthranilic acid, in dye decolorization by Fenton processes," *Int. Biodeterior. Biodegradation*, vol. 104, pp. 1–7, 2015. Available: doi: 10.1016/j.ibiod.2015.05.007.

[29]   F. Barreto, C. S. Santana, and A. Aguiar, "Behavior of dihydroxybenzenes and gallic acid on the Fenton-based decolorization of dyes," *Desalin. Water Treat.*, no. October 2014, pp. 1–19, 2014. Available: doi: 10.1080/19443994.2014.966333.

[30]   P. K. Malik and S. K. Saha, "Oxidation of direct dyes with hydrogen peroxide using ferrous ion as catalyst," *Sep. Purif. Technol.*, vol. 31, pp. 241–250, 2003.